Environmental Modelling and Software 173 (2024) 105955

Contents lists available at ScienceDirect

Environmental Modelling and Software

journal homepage: www.elsevier.com/locate/envsoft

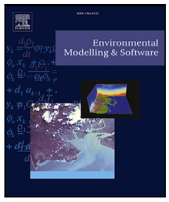

MitH: A framework for Mitigating Hygroscopicity in low-cost PM sensors

Martina Casari *, Laura Po

"Enzo Ferrari" Engineering Department, University of Modena and Reggio Emilia, Modena, Italy

ARTICLE INFO

Keywords:
Air quality
PM
Low-cost sensors
Mitigate Hygroscopicity
Dynamic
Real-time

ABSTRACT

Air quality estimation using low-cost sensors is a pressing issue, with meteorological factors often causing measurement discrepancies. Hygroscopicity, arising from humidity's interaction with particulates, leads to inaccurate PM concentration readings in laser-scattering low-cost PM sensors. Common remedies involve data removal during high relative humidity or reference station calibration, but these solutions are not always practical or accurate due to the localized nature of hygroscopicity. In this paper, the authors present an adaptive correction framework that dynamically models hygroscopicity effectively mitigating humidity's impact on particle measurements. The framework exploits historical sensors' data, providing real-time adaptability in any context without relying on reference data, thus improving air quality estimations from low-cost sensors.

1. Software and data availability

Name of the software: MitH (**Mit**igate **H**ygroscopicity) Framework
Developer: Martina Casari, Laura Po
Contact information: martina.casari@unimore.it, laura.po@unimore.it
First-year available: 2023
Program language: Python
Cost: free
Software availability and open data: https://gitlab.com/martina.casari.93/sensordatacorrection-hygroscopicity.
Program size: less than 2MB

2. Introduction

Air pollution is a growing concern in many countries, fuelled by factors such as increased industrial activity, transportation, and urbanization. The impact of air pollution has well-documented adverse effects on public health, including respiratory problems, heart disease, stroke, and lung cancer (Zhu et al., 2019; Rajagopalan et al., 2018; Verhoeven et al., 2021; Xue et al., 2022; Kiesewetter et al., 2015). Additionally, it contributes to global warming, acid rain, and environmental degradation. As a result, there is an urgent need for sustainable solutions to mitigate air pollution and the use of low-cost sensors (LCS) to monitor air quality is a promising approach (Campo et al., 2023; Coker et al., 2022; Amegah, 2018; Amegah et al., 2022; Barkjohn et al., 2021; Int Panis et al., 2010). Moreover, the availability of multiple air quality control dashboards, including mobile applications, has significantly increased public awareness and engagement in monitoring and improving air quality (Kelly et al., 2023; Zafra-Pérez et al., 2023; Kosmidis et al., 2018).

While LCS have become increasingly popular due to their affordability and portability, their limited technology may not meet regulatory standards for quantitative evaluation (WHO et al., 2021; Sá et al., 2022). However, when aggregated for citizen science purposes, they can complement reports from governmental agencies, improving spatial resolution (Apte et al., 2017).

The detection of particulate matter (PM) levels is of utmost importance in environmental monitoring and public health. PM refers to tiny particles suspended in the air, which can include various pollutants such as dust, smoke, soot, and aerosols. These particles can have detrimental effects on human health when inhaled, especially PM2.5 (particles with a diameter of 2.5 micrometres and smaller) which can penetrate deep into the respiratory system. In the atmosphere, particles can originate from both direct emissions and secondary formation processes. Direct emissions refer to particles that are emitted directly from specific sources such as construction sites, unpaved roads, fields, smokestacks, or fires. Industrial facilities, power plants, and vehicles mainly generate these primary pollutants. On the other hand, secondary pollutants are formed through complex chemical reactions that take place within the atmosphere (Chang and Lee, 2007; Li et al., 2017; Siciliano et al., 2021; Dimitriou et al., 2023).

Apart from meteorological influences (Danek et al., 2022), one of the most significant limitations of LCS in measuring PM is their sensitivity to humidity (Jayaratne et al., 2018). This is because particles present in the atmosphere may absorb water and increase in size, leading to an overestimation of the PM concentration detected by the

* Corresponding author.
E-mail addresses: martina.casari@unimore.it (M. Casari), laura.po@unimore.it (L. Po).

https://doi.org/10.1016/j.envsoft.2024.105955
Received 11 August 2023; Received in revised form 18 December 2023; Accepted 9 January 2024
Available online 10 January 2024

sensor. This is known as the hygroscopic property of the particle. High humidity can also cause false readings due to the formation of water droplets, leading to inaccuracies in measurements (Skupin, 2013; Molnár et al., 2020; Hagan and Kroll, 2020; Crilley et al., 2018; Manikonda et al., 2016). This is especially problematic for laser-based sensors, which measure particle size and concentration using laser scattering. It is important to highlight that water vapour is not harmful to human health. Therefore, it is essential to model and remove this artefact to obtain accurate pollution level measurements comparing the LCS measurements with regulatory station measurements. As a matter of fact, the EU air quality standards (EEA, 2021), the WHO air quality guidelines (WHO et al., 2021), and other governmental organizations, measure pollution impact based on the dry PM concentration.

To ensure accurate measurements with LCS, researchers and manufacturers have developed procedures and algorithms to mitigate the effects of relative humidity (RH) and improve sensor design. Typical corrective methods utilized measurement data and a reference station to estimate corrective function or regression model parameters for relative humidity correction, or integrated a dryer into the sensor to counteract the effects of humidity (Owczarek et al., 2020; Laquai and Kroseberg, 2021; Zusman et al., 2020; Giordano et al., 2021; Shi et al., 2017; Di Antonio et al., 2018; Hofman et al., 2022b).

For low-cost PM sensors where integrating a dryer is not feasible, existing approaches face significant limitations, primarily due to their heavy reliance on time and location (Streibl, 2017; Rogulski and Badyda, 2020). Methods trained in one location may not accurately capture the environmental specifics when the sensor is moved to a different location, requiring parameter adjustment and re-training (Crilley et al., 2020; Jin et al., 2022). Additionally, methods that require LCS to be stationed near reference stations for prolonged periods limit their practical use for other applications. Furthermore, approaches based on the *k*-Köhler theory rely on knowing the elemental analysis of the air, which may not always be readily available or subject to frequent changes, limiting their applicability in certain scenarios.

This paper aims to overcome these limitations and develop a more versatile framework. The Mitigating Hygroscopicity (MitH) framework can effectively model the hygroscopicity effect and is available as open-source software.

MitH excels with its dynamic adaptability, managing anomalies effectively. It operates independently of reference stations, making it versatile in diverse environments. MitH's real-time capabilities offer practical solutions for hygroscopicity challenges in both real-world applications and research.

Thanks to its distinctive features, MitH framework offers valuable advantages. It enables the evaluation of modelled air quality data across a larger number of locations, overcoming the limitations of conventional simulation techniques that heavily rely on data from reference stations or high-precision sensors (Brusseleers et al., 2023; Hofman et al., 2022a). Moreover, integrating MitH into interpolation techniques allows for the incorporation of more accurate air quality data, resulting in more comprehensive and representative modelling outcomes. Furthermore, MitH's effectiveness in visualizing and managing environmental sensor data provides valuable insights into air quality patterns and trends. This supports informed decision-making and environmental management (Horsburgh et al., 2015).

It is important to note that while MitH addresses the specific challenge of hygroscopicity, it does not negate the need for calibration techniques in LCS. It is acknowledged that sensors can encounter various limitations, such as sensor drift, ageing, temperature sensitivity, cross-sensitivity to other pollutants, and inherent measurement biases. These factors can introduce errors and inaccuracies in the sensor readings. Therefore, it is crucial to incorporate appropriate calibration techniques to account for these factors and ensure accurate and reliable measurements (Giordano et al., 2021; Zhivkov, 2021).

The rest of the paper is structured as follows. In Section 3, the study site, data collection, data pre-processing, parameter optimization and the application of the corrective functions are explained in detail. Section 4 is dedicated to the evaluation of the proposed approach. Various study highlights are presented, such as an analysis of anomalous sensors, the examination of parameter choices, and the performance evaluation of each module's step of the approach. Furthermore, a comparison with existing approaches is provided. The Discussion section delves into a detailed analysis and interpretation of the results, providing deeper insights into the findings (refer to Section 5). Finally, Section 6 wraps up the article, summarizing the main outcomes and implications of the study.

3. MitH framework

The main features of MitH are:

- **Anomalies-tolerant.** The framework can effectively handle anomalies in the data it processes (Russo et al., 2020; Jones et al., 2022). It identifies, removes and replaces outliers and spikes from sensor data.
- **Dynamic and adaptable.** This approach allows for continuous updates and refinements of the corrective function, thanks to rolling window data, making it context-aware and capable of accommodating variations across different environments, also in isolated and humid locations, where traditional calibration techniques may be limited.
- **Reference station-agnostic.** Unlike existing approaches that require LCS to be stationed near reference stations for extended periods, MitH framework can be applied in any context, boosting its usability, also when calibration is challenging or when a model is not exploitable due to different environmental conditions.
- **Real-time.** By providing timely and context-aware corrections, MitH offers a practical and efficient solution to address the hygroscopicity challenge in real-world applications and research endeavours (Hill and Minsker, 2010).

MitH is organized into four modules, as illustrated in Fig. 1, along with a final evaluation step:

(a) *Data collection*: In the first module, data are collected from LCS. Each subsequent module is performed separately for each sensor's data.
(b) *Data pre-processing*: In this module, the chosen $process\_mode$ and $window\_size$ values are utilized to pre-process the operational window, composed by the new observation(s) and the relative window history. This pre-processing aims to eliminate any significant statistical anomalies present in the data.
(c) *Parameter optimization*: The third module involves optimizing the parameters of the corrective function. This optimization is carried out to ensure that the function accurately captures the relationship between relative humidity and particulate matter based on the operative window data obtained from the previous module. As a result, the function is context-aware. The optimal parameters obtained during this optimization are retained for the next module use.
(d) *Application of the correction function*: In the final module, the optimized corrective function is applied to the newly measured data, in which RH is above a certain threshold. This application serves to correct any potential hygroscopic biases caused by humidity in the particulate matter measurements.

Upon completion of the four MitH modules for each sensor, a conclusive assessment is conducted by comparing the corrected observations with those obtained from the reference station. It is important to note that the reference observations are exclusively used at this stage; they are not employed in either the optimization or correction phases. Indeed, the framework refines sensor observations without relying on any reference data.

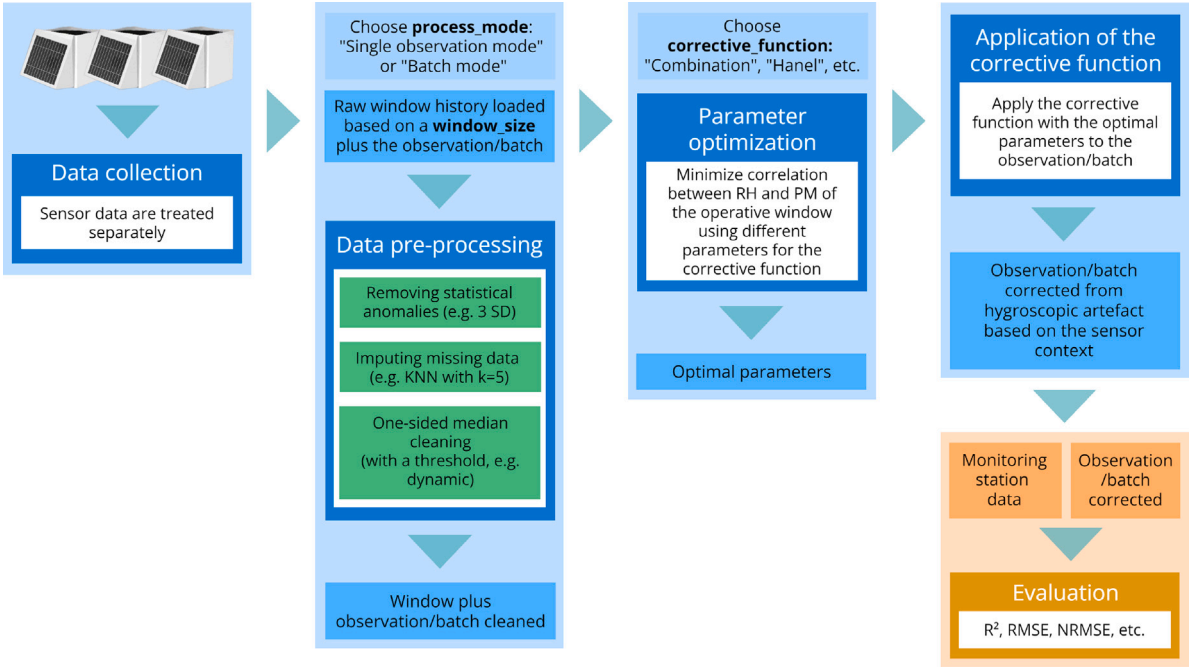

Fig. 1. Flowchart displaying the presented MitH (Mitigating Hygroscopicity) framework, which consists of four main modules: data collection, data pre-processing, parameter optimization, and application of the corrective function.

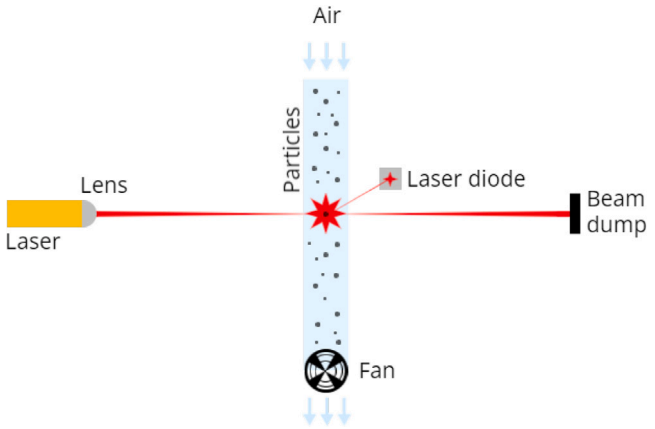

Fig. 2. The operational mechanism employed by the Sensirion SPS30 low-cost air quality sensor.

3.1. Study site and data collection

The air quality data were collected using the Arianna devices developed by Wiseair,[1] a Milan-based start-up that aims to enhance policies related to air quality standards. The Arianna devices are equipped with a Sensirion SPS30 and an integrated solar panel to function, meaning that they rely on sunlight to generate the necessary power to operate. Sensirion SPS30.[2] sensor uses a laser scattering measurement principle with contamination-resistance technology and is compliant with MCERTS Performance Standards for Indicative Ambient Particulate Monitors (Version 4 dated August 2017)[3]

When it comes to low-cost laser scattering sensors, they can be broadly classified into two categories: volume scattering or integrating nephelometers and single particle counters. The SPS30 sensor is an optical particle counter (OPC) (see Fig. 2), which is a type of single particle counter widely used for counting particles in the range of 0.25 μm to several microns. OPCs use laser scattering technology to measure the amount of light scattered by individual particles as they pass through a beam of light. A portion of the scattered light is collected and directed to a photodetector, where it is converted to a voltage pulse. Particle size is then determined from the magnitude of this voltage pulse using a calibration curve (Sousan et al., 2021). These sensors can convert the electrical signal into different size concentrations of the various PM and the number of particles detected for each bin (see Table 1), even with a small sample airflow and a short measurement time. The SPS30 sensor utilizes unique contamination resistance technology that ensures the optics remain clean and maintenance-free throughout its lifetime. However, the Arianna devices lack a drying function, and thus the collected data can be affected by humidity levels, even if the sensors are operated within the recommended humidity range of up to 80% (see Table 2).

The comparison of PM concentrations measured by LCS with and without the dryer indicates that it can effectively dry out the water vapours generated from the vaporizer (Samad et al., 2021). Unfortunately, it is not possible to incorporate a dryer into the Arianna device due to limitations with the power supply from the solar panel.

The study was conducted in Turin, Italy, which is the capital city of the Piedmont region in northern Italy. Turin has a population of approximately 847,000 inhabitants and covers an area of 130 square kilometres. In 2019, Wiseair initiated a Citizen Science project in Turin to increase awareness among the city's population regarding pollution levels. As part of this project, over 20 Arianna devices were strategically deployed across the city. Some of these devices were co-located close to a reference station operated by Arpa (the regional environmental protection agency), situated in a public garden, away from heavy traffic (see ARPA-Torino (2023) for topology specification). The reference station is a Tecora Sequential Unit, that utilizes gravimetric technology, enabling accurate measurements of PM10 and PM2.5 concentrations. The low-cost devices were positioned on the perimeter fence surrounding the reference station, elevated at a height of 4 m.

[1] https://wiseair.vision/
[2] https://sensirion.com/products/catalog/SPS30/
[3] https://sensirion.com/media/documents/3A3BF572/616540E1/Sensirion_PM_Sensors_Datasheet_SPS30_MCERTS-Certificate_2020.pdf

Table 1
Particulate matter SPS30 sensor specifications.

Parameter	Conditions	Value	Units
Mass concentration range	–	0 to 1000	$\mu g/m^3$
Mass concentration size range	PM1.0	0.3 to 1.0	µm
	PM2.5	0.3 to 2.5	µm
	PM4	0.3 to 4.0	µm
	PM10	0.3 to 10.0	µm
Mass concentration precision for PM1 and PM2.5	0 to 100 $\mu g/m^3$	±10	$\mu g/m^3$
	100 to 1000 $\mu g/m^3$	±10	%m v.
Number concentration precision for PM0.5, PM1 and PM2.5	0 to 1000 $\#/cm^3$	±100	$\#/cm^3$
	1000 to 3000 $\#/cm^3$	±10	%m v.
Lifetime	24 h/day operation	>10	years
Maximum long-term mass concentration precision limit drift	0 to 100 $\mu g/m^3$	±1.25	$\mu g/m^3$/year
	100 to 1000 $\mu g/m^3$	±1.25	%m v./year

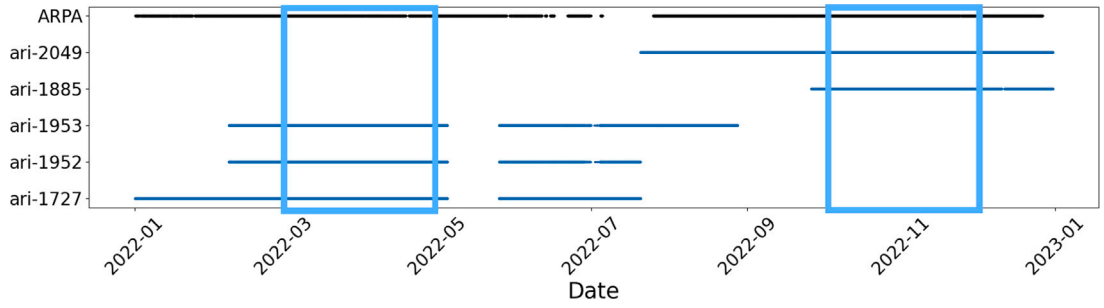

Fig. 3. Operating periods of LCS and ARPA reference station in 2022.

Table 2
SPS30 recommended operating conditions.

Parameter	Recommended Operating Conditions
Temperature	10 to 40 °C
Relative humidity	20 to 80%

The Arpa reference station provides hourly data of validated PM 2.5 levels. The agency conducts the validation using the medium bound technique, estimating concentrations below the detection limit as half of the detection limit for the target substance. In contrast, the Wiseair Arianna devices collect data at 15-minute intervals. Wiseair has its own corrective algorithm, which includes a threshold, a correction function with fixed parameters, and a regression applied for the autumn season. In this study, the data used are the raw ones. A detailed comparison between the proposed approach and Wiseair's is provided in Section 4.5.1. Despite the 15-minute frequency, the data collection frequency is influenced by factors such as the battery level, contingent on the sunlight received by the solar panel. The final evaluation is conducted hourly to match the Arpa reference station granularity, taking an hourly mean of the data collected from each sensor.

The study was conducted over two distinct periods. The first period took place from March to April 2022, during spring. The second period occurred from October to November 2022, representing autumn. By analysing data from both seasons, the study aimed to capture variations in RH levels and evaluate the performance of LCS under different environmental conditions. During these specific periods, multiple LCS were available for comparison with the Arpa reference station. The activity of the sensors is illustrated in Fig. 3. Despite having a more extended duration for data collection in the autumn period, the decision was made to use an equal amount of time for both periods, ensuring consistency and comparability.

A total of 13,000 observations were collected from five Arianna devices. The devices provided a comprehensive set of data, including various environmental parameters and pollutant concentrations. The recorded data from the Arianna devices consisted of the following variables for each observation: date and time in UTC, temperature in degrees Celsius, relative humidity in percentage, pressure in hPa, cloud coverage in percentage, wind speed in metres per second, wind direction in degrees, and concentrations of PM1, PM2.5, PM4, and PM10 in micrograms per cubic metre ($\mu g/m^2$). On the other hand, the reference station operated by ARPA provided a dataset of 3000 hourly measurements. The data included date and time in GMT+1 and measurements of NO2, NO, NOx, PM10, and PM2.5 concentrations in micrograms per cubic metre ($\mu g/m^2$).

As it is well-known, larger diameter particles encompass smaller ones. Specifically, PM10 includes particles with lower diameters, while PM4 includes PM2.5 and PM1, and PM2.5 includes PM1. In the current study, the focus was exclusively on PM2.5, because the SPS30 sensor provides more precise measurements for this particular particle size compared to PM10. Additionally, PM2.5 particles are known to be more harmful to human health.

3.2. Data pre-processing

The pre-processing is applied to the new observation(s) along with its historical window. If there is only one observation, in the study is referred to as *single observation mode*, and if there are multiple observations, as *batch mode*. In both cases, the new observation(s) undergo preprocessing together with the preceding historical window of length $window\_size$. This combined window, consisting of the historical window and new data, is now referred to as the operative window (see Fig. 4).

Excluding the single observation/batch into the context used in the pre-processing and optimization is possible even if not recommended.

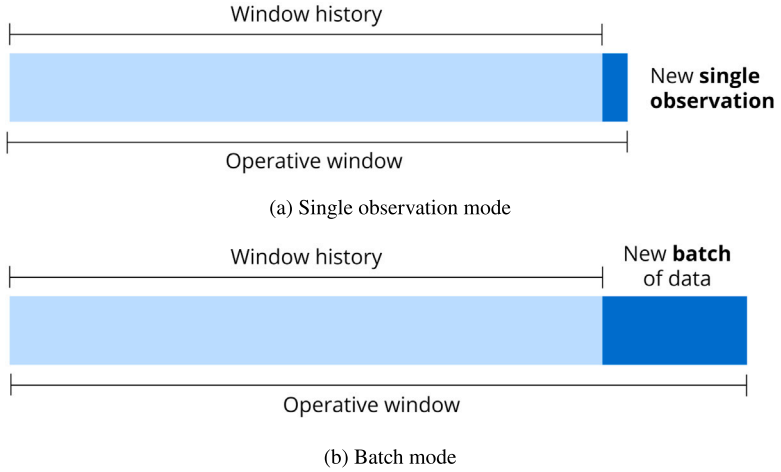

Fig. 4. Two different approaches for data pre-processing and optimization modules: considering each observation individually during pre-processing and optimization (a), or processing multiple observations simultaneously as a batch (b).

By excluding the new data, the operative window is equivalent to the window history. In the *single observation mode*, the downside of not keeping them is less evident because the window history is more similar to the operative window. In the *batch mode*, the window history itself could not be enough to explain the context of the new observations. Section 4.3 shows what happens when the batch data context is excluded from the operative window.

The preprocessing considers various factors, including the identification and removal of statistical anomalies, imputation of missing data using the k-Nearest Neighbours (KNN) method, and a one-sided median cleaning process for correcting right-skewed data. These steps are tailored to enhance the data quality and prepare an operative window for further analysis.

After having chosen the $processing\_mode$, as a single observation or batch, and the $window\_size$, the pre-processing is performed over the data loaded. The pre-processing, as illustrated in Fig. 1 second box, is composed of three phases:

1. *Removing statistical anomalies*: The phase involves identifying anomalies in the data by calculating the standard deviation and replacing any events that fall outside 3 standard deviations with NaN values. This helps to eliminate rare and unlikely data points, which are likely to be caused by a misreading of the sensor. It is worth noting that this step might raise concerns, especially considering that high values are crucial when studying hygroscopicity. However, a prior analysis of the raw data revealed rare and very high peaks, exceeding 1000 $\mu g/m^3$. These peaks are not indicative of concentrations affected by hygroscopicity, but rather anomalous data. Applying a 3-standard deviation threshold helps retain peaks induced by hygroscopicity while removing anomalous peaks caused by device errors. Alternatively, a threshold could be used if prior knowledge is available. When handling raw data unaffected by humidity, setting a threshold becomes more straightforward, especially when there is a reference limit for PM data available. However, in the hygroscopic environment, determining a suitable threshold is challenging due to the lack of prior knowledge regarding the maximum concentration levels detectable. Therefore, the 3-standard deviation approach is considered appropriate for filtering out only anomalous peaks, where "anomalous" does not refer to hygroscopicity-induced values but rather to exceptional values.
2. *Imputing missing data*: The second phase is filling in any missing data points. This is done by replacing the NaN values using a k-Nearest Neighbours (KNN) imputation method with a chosen k-value. This results in a minor loss of data points and the missing data are refilled using similar contexts. Of course, the imputation algorithm could be chosen from the classic set of filling algorithms. The choice reflects the capacity of the KNN to use any other available variables (described in Section 3.1) to fill empty values.
3. *One-sided median cleaning*: The final phase is a one-sided median cleaning process, which is used to correct right-skewed data. A sliding window is used to determine the median value of the data. Any data points that fall outside the median plus a calculated threshold are replaced with the median value of the window. In the study, the threshold is calculated using statistical properties of the available data, but it should also be determined based on other environmental-specific knowledge. This process is performed only on the right side of the data, hence the term "one-sided" median cleaning, to ensure a real-time approach. It is important to note that the window used should be a temporal arch and not a number of preceding observations unless the frequency of reading of the sensor is ensured.

During each phase, adjustments can be made to various parameters. This includes the standard deviation in the first phase, the k-value used in the KNN algorithm, in the second phase, and the number of hours of the rolling window and the threshold in the last phase.

It is important to note that after the removal of anomalous data during pre-processing, the data may not include certain events, for instance, fires, that initially appear as anomalies and are subsequently modified during pre-processing. As time passes and the event persists, the data that were initially considered anomalous may no longer be considered as such and become useful for building a more accurate context. However, this possible delay must be taken into consideration.

As depicted in the flowchart, at the conclusion of the pre-processing, the process yields an operative window cleared of significant statistical anomalies.

3.3. Parameter optimization

After the completion of the three pre-processing steps, the historical data window is ready for the corrective function optimization. Various corrective functions, often referred to as growth functions, have been proposed in the literature to address the issue of hygroscopicity (Day and Malm, 2001; Gurumurthy Ramachandran and Sexton, 2003; Christakis et al., 2022). These functions are designed to calculate a corrective coefficient that can be applied to reduce the concentration level of particulate matter based on the relative humidity level, as in Eq. (1).

$$PM_{dry} = \frac{PM_{wet}}{gf(RH)} \tag{1}$$

The PM results are said corrected with respect to the problem of hygroscopicity. In the equation, PM_{wet} represents the PM concentration detected by LCS and PM_{dry} represents the PM concentration after the application of the growth function gf.

In Streibl (2017) a list of possible corrective functions is presented, among with the *Hänel* (Eq. (2)), and a new proposal called Combination (Eq. (3)).

$$gfhanel = \frac{1}{(1-RH)^{\beta}} \tag{2}$$

$$gfcombo = 1 + \alpha \cdot \frac{RH^2}{(1-RH)^{\beta}} \tag{3}$$

Soneja et al. (2014) provide two other corrective functions, the first proposed in Chakrabarti et al. (2004), call *Chakrabarti* equation (Eq. (4)) and the second, *Richards*'s humidity adjustment (Eq. (5)), originally proposed in Richards et al. (1999).

$$gfchakrabarti = \alpha + \beta \cdot \frac{RH^2}{1-RH} \tag{4}$$

$$gfrichards = exp(\alpha + \beta \cdot Ln(1-RH)) \tag{5}$$

Streibl's work provides insights into the different behaviours of corrective functions optimized over months. He also emphasizes the importance of pre-processing, which is similar to the one applied in this study. That is, in the pre-processing module phases, a range was used to reduce anomalies instead of SD, and a non-context-aware algorithm was employed in the filling algorithm. The final phase involved a median window smoother, although details were not provided.

Regarding the optimization of the corrective function, Streibl argues that since RH and PM are not correlated in reality, two possible approaches can be considered:

1. Minimizing the Fourier coefficient: This approach takes into account the periodic component with a 24-hour period present in temperature, humidity, and particulate matter growth. By minimizing the absolute value of the corresponding normalized Fourier coefficient, the influence of humidity can be compensated to the best possible extent.
2. Minimizing the correlation factor: This approach aims to minimize the correlation between the corrected PM and RH. By achieving a minimal correlation, the influence of humidity can be effectively compensated.

In the case of *Chakrabarti* and *Richard*'s equations, Soneja et al. explored the original parameters proposed in *Chakrabarti*'s original work for the first, as well as new parameters fitted using simulated cooking test data for both. Additionally, they compared the application of these three corrective functions to the entire dataset versus applying them only to data above a certain threshold. The findings suggested that using a threshold for applying the corrective functions was a better approach. Furthermore, it was observed that a threshold of 60% relative humidity appeared to be generally too low.

Typically, as for Soneja, the optimization process involves finding the values of the corrective function that provide the best match between the observed data and the reference station values. Once the corrective function has been optimized, it is used to correct the raw sensor data. This fitting procedure relies on the fact that the optimal parameters for a specific context are explanatory in general.

In contrast, MitH does not rely on the use of a reference station to optimize the parameters of the corrective function. Instead, two distinct approaches were explored. The first approach involved minimizing the correlation between relative humidity and particulate matter measurements, as suggested in Streibl. The second approach focused on minimizing the difference between the distribution of the original data below a chosen threshold and the data corrected above the same threshold.

Two real examples of parameter optimization modules, based on the correlation minimization approach, are shown in Fig. 5. The x-axis, which remains the same among the two subplots, represents the combined parameters used for optimization, and the y-axis represents the correlation obtained. The figure highlights two different periods, to demonstrate the difference in parameter selection even for closely spaced time periods.

Given a curve, it is possible to see how different corrective function parameters yield different correlation values between RH and PM; the same happens when using the distribution difference minimization approach. In the figure, it is evident that there exists an optimal point where the correlation is minimized, which is the one obtained with the parameters used as optimal in the next module. Consequently, by applying the correlation (or distribution difference) minimization over the operative window, the corrective function can be customized to the specific characteristics of the sensor and account for the impact of relative humidity on the sensor readings within the specific environmental context. As a result, this dynamic approach enables MitH to effectively adapt to environmental changes over time, without the need for a reference station.

To effectively implement this approach, there is a prerequisite for a significant volume of historical data to ensure the precise optimization of the corrective function. This entails periodic reevaluation of the parameters involved in the correction process. Despite these demands, the approach proves especially beneficial for LCS that may lack access to reference station data for calibration.

3.4. Application of the corrective function

In the fourth module of the process, the optimal corrective function found is applied as a corrective coefficient to the current observation(s), as in Eq. (1), if the associated relative humidity is above a certain threshold. As a result, the corrected data provides a more accurate representation of the particulate matter levels, compensating for the influence of humidity on the sensor readings.

After obtaining the corrected data, the evaluation was conducted by comparing them to the data received from the Arpa reference station. The evaluation was performed using metrics such as R^2, RMSE, and NRMSE. It is noteworthy that the granularity of the data remained consistent with that collected by LCS, approximately every 15 min, during the evaluation process. However, for the purpose of comparison with the measurements from the Arpa reference station, the data were re-sampled to reflect the hourly granularity imposed by the reference station. This adjustment facilitated a meaningful assessment of the accuracy of the MitH framework.

4. Results

In this section, several key insights are presented, focusing on evaluating the performance of MitH. The results section is divided into the following subsections to provide a comprehensive analysis:

1. *Sensors Behaviour Analysis*: An examination of the behaviour of sensors during the corrective process, aiming to identify specific patterns or challenges encountered (see 4.1).
2. *Window History Size*: Exploration of the impact of different window history sizes on the performance of the corrective function. This involves assessing how the choice of $window_size$ influences the accuracy of the corrected data (see 4.2).
3. *Context Inclusion*: Discussion of the advantages of including the context of new observations alongside the window history in the parameter optimization process. Incorporating current environmental conditions aims to enhance the accuracy of the corrective function (see 4.3).
4. *Step Performance*: Evaluation of the performance at different stages of the approach, including raw data, pre-processed data, and corrected data (see 4.4).

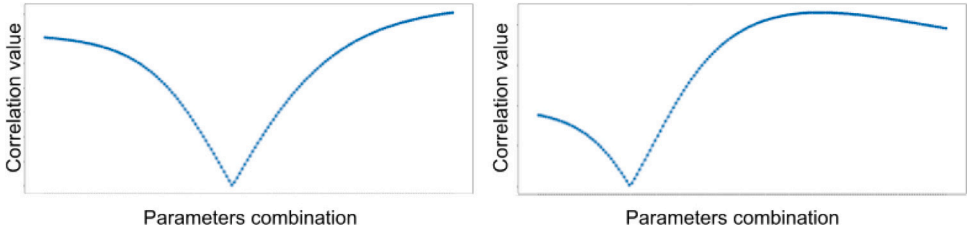

Fig. 5. Two real examples of parameter optimization for reducing Relative Humidity correlation to Particulate Matter concentration levels.

5. *Comparison with Existing Approaches*: Presentation of the results of the presented approach and a comparison with outcomes achieved by applying approaches described in the literature (see 3.3). This comparison provides insights into the effectiveness of MitH in addressing the hygroscopicity issue and improving the accuracy of sensor data (see 4.5).
6. *Wiseair approach comparison*: In the last subsection, a comparison is provided between the Wiseair corrective method approach and MitH.

The presentation of these subsections aims to offer a comprehensive understanding of the performance and effectiveness of the proposed approach in addressing hygroscopicity in low-cost sensor data.

In the following, the application results are presented in terms of RMSE (Root Mean Squared Error), NRMSE (Normalized Root Mean Squared Error), and R^2. Additionally, some of the results are visualized as time-series plots to demonstrate practical outcomes and capture some peculiarities of the process. The evaluation metrics, such as RMSE and NRMSE, provide quantitative measures of the model's performance in terms of accuracy, estimating how well the model can predict the target value. A lower RMSE and NRMSE indicate better agreement between the corrected values and the ground truth, in addition, NRMSE may be useful to make the evaluation scale-free. Furthermore, the R^2 value assesses the goodness of fit of the corrected data compared to the observed data. A higher R^2 value indicates a stronger correlation and better predictive capability of the correction model.

4.1. Sensors behaviour analysis

An important aspect to consider when working with LCS is that they can exhibit a wide range of anomalies. Fig. 6 clearly demonstrates this phenomenon, where the sensor labelled ari-1727 (the blue line) consistently shows higher concentration levels compared to the other sensors. This discrepancy is visually evident in the plot, as the data from ari-1727 consistently deviates from the overall trend observed in the other sensors (orange and green lines), which approximates the reference station (black line) better.

Although some peaks are reduced after pre-processing (see subfigure b), the overall signal from the ari-1727 sensor remains compromised. Moreover, such anomalies are not addressed by the corrective function used in this study, as the RH threshold chosen for correction is higher than the RH levels detected during these measurements. This suggests that the observed anomaly is likely unrelated to hygroscopic effects. Consequently, addressing this anomaly would require additional pre-processing steps specifically designed to handle such anomalies. It is important to mention that despite these anomalies, the sensor remains useful as it generally aligns with PM concentrations from other sensors for the majority of the time, justifying its inclusion in the study.

However, this emphasizes the complexity and challenges associated with correcting and processing data from LCS, especially when dealing with anomalous sensor behaviour. Further investigation and refinement of pre-processing techniques may be necessary.

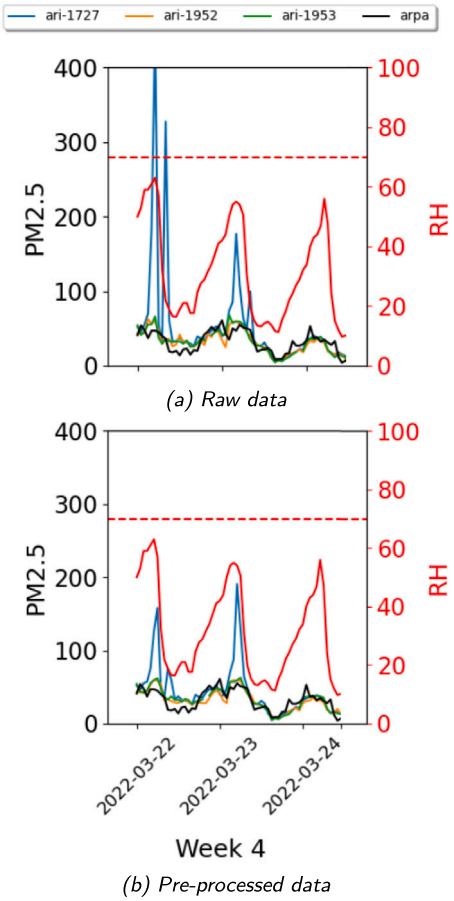

Fig. 6. Anomalous sensor behaviour with elevated concentration levels: Raw data with visually prominent readings (a) and cleaned data after pre-processing (b).

4.2. Window history size

The choice of the $window\_size$ parameter is crucial in contextualizing the corrective function and obtaining optimal corrective parameters for the specific period under consideration. Initially, it was believed that a larger window size would lead to better performance. However, the findings contradict this assumption.

It has been observed that a shorter window history is sufficient to optimize the corrective function parameters, and using longer window periods diminishes performance. This is illustrated in Table 3, where the performance metrics are plotted against different window sizes. The performance of LCS is evaluated by comparing the sensors' concentration with the reference station for both the spring measurement period and the autumn measurement period.

The results demonstrate that a briefer window history (12 h or 1 day) yields better results in terms of corrective parameter optimization. However, it was observed that if the window history is too short, it may

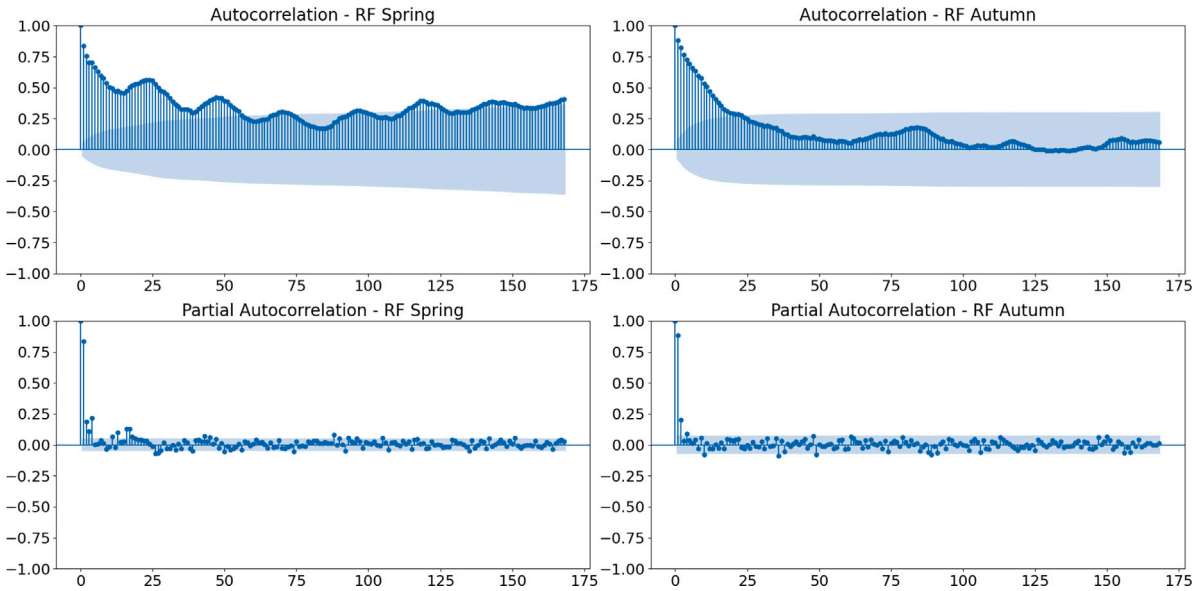

Fig. 7. Autocorrelation and partial autocorrelation plots for hourly PM2.5 concentrations at the reference station.

Table 3
Comparison of LCS performance with reference station across varying window sizes - Parametersfixed in the comparison: batch dimension of 1 day, optimization method correlation minimization, corrective function *Combination*, RH threshold 70%.

Window size	Spring period			Autumn period		
	R^2	RMSE	NRMSE	R^2	RMSE	NRMSE
12 h	0.778	**11.132**	**0.505**	0.626	12.219	0.573
1d	**0.781**	11.157	0.506	**0.636**	**12.010**	**0.563**
2d	0.779	11.231	0.509	0.577	12.766	0.598
1w	0.776	11.577	0.525	0.543	14.378	0.674
2w	0.760	11.749	0.533	0.577	13.751	0.644
3w	0.702	12.866	0.583	0.549	14.104	0.661

not contain enough representative context data, including the classical cyclic relative humidity pattern. This observation is particularly relevant when the process mode is set to *single observation mode*. On the other hand, if the *batch mode* is preferred and a sufficiently large batch is used, these issues can be mitigated to some extent. Therefore, the choice of process mode and the size of the batch can have an impact on the effectiveness of the corrective parameter optimization if a small $window\_size$ is used.

An additional interesting insight can be extracted from the examination of the autocorrelation (ACF) and partial autocorrelation (PACF) plots above hourly PM 2.5, during both the spring and autumn seasons. In Fig. 7, the disparities in ACP between spring and autumn regarding PM2.5 concentrations likely arise from variations in environmental conditions, human activities, and seasonal influences. During spring, a noticeable seasonal pattern after one day may signify cyclic environmental events. Conversely, autumn lacks a discernible seasonal pattern, and there is a swift decline in autocorrelation after one day, indicating a more dynamic and responsive system.

It is noteworthy that, despite the observed seasonal ACF in spring, the PACF plot suggests that employing a window size of 1 day might be adequate for optimizing meaningful contextual insights. However, considering the observed dynamics, exploring a dynamic window based on the season could be a valuable option for further investigation.

4.3. Context inclusion

The decision to include or exclude the observation(s) to be corrected, along with their corresponding relative humidity levels, during the optimization step of the corrective function can significantly affect the obtained results. It is important to note that when the process mode is set to batch and the observations are not included in the operative window (as shown in the *batch mode* Fig. 4), there is a contextual information gap. This means that the overall context for the entire batch is missing, which can potentially result in a less accurate outcome. However, when the correction process is performed for each new observation, in the *single observation mode*, the impact of non-inclusiveness is reduced. This is because the historical data used for each observation is more closely related and relevant to the specific context of that individual observation.

Importantly, it should be clarified that including new data does not equate to using redundant, inappropriate information, or introducing bias. On the contrary, it is vital to ensure the improved performance of the corrective process.

In this study, a comparison between the two approaches was conducted. Specifically, the *Combination* function was applied to the data both with and without incorporating the observation(s) to be corrected during the pre-processing and parameter optimization steps. Fig. 8 illustrates the differences in the results.

In subplot (a), the presence of the plateau observed in subplot (b) is not evident. This discrepancy can be attributed to the difference in the context considered during the parameter optimization. When the optimization technique was applied to the whole batch at the same time, on day 2022-03-30 (batches of 24 h were utilized), the previous period (window history) did not experience an RH greater than 70%. Consequently, the corrective function lacked optimization for the upper range of RH thresholds. This led to the corrective coefficient potentially exhibiting an overly aggressive impact upon application However, by including the observations to be corrected during the pre-processing and parameter optimization steps, this negative effect was reduced. Therefore, the more comprehensive context provided by including the relevant observations resulted in a more accurate correction.

4.4. Modules' steps performance

During the evaluation process, the results were analysed at different stages of the correction process, namely raw data, pre-processed data, and corrected data (see Table 4). R^2, RMSE and NRMSE values were calculated for each module's step, and the results were presented separately for each sensor, comparing the concentration data from these sensors with those from a reference station, enabling a thorough assessment of their performance across different periods.

Table 4
Evaluation of LCS data during spring (a) and autumn (b) periods.

(a) Spring period

Sensor ID	Raw data			Pre-processed data			Corrected data		
	R^2	RMSE	NRMSE	R^2	RMSE	NRMSE	R^2	RMSE	NRMSE
ari-1727	0.562	29.440	1.335	0.631	25.261	1.145	0.724	14.138	0.641
ari-1952	0.599	22.877	1.037	0.601	22.927	1.039	0.810	9.552	0.433
ari-1953	0.554	26.908	1.220	0.558	27.269	1.236	0.809	9.782	0.443

(b) Autumn period

Sensor ID	Raw data			Pre-processed data			Corrected data		
	R^2	RMSE	NRMSE	R^2	RMSE	NRMSE	R^2	RMSE	NRMSE
ari-2049	0.177	116.174	5.444	0.168	115.019	5.390	0.647	12.600	0.590
ari-1885	0.232	75.202	3.524	0.218	74.798	3.505	0.625	11.419	0.535

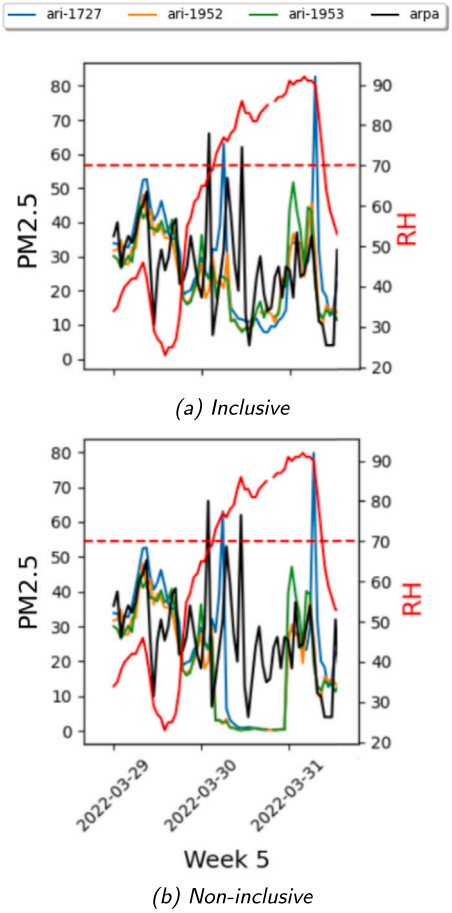

Fig. 8. Comparison of correction approaches within the same time frame: by incorporating new observations in the operative window (a), and without the incorporation of new observations (b).

One notable finding from the evaluation is the beneficial impact of the pre-processing on anomalous sensors, such as ari-1727. These sensors exhibited improved performance after undergoing this step. However, for other sensors, the pre-processing did not yield significant improvements in the results. Its impact on their performance was relatively low.

In Fig. 9 a comparison is presented between the raw data and the pre-processed and corrected data, displaying four weeks of data collected from LCS and the reference instrument (Arpa) at the monitoring site in Torino. The data for each week is presented as a time series, with the black line representing the reference instrument and LCS shown in different colours. The red line on the graph represents the level of relative humidity, with a dotted threshold of 70% RH shown.

During the analysis of the data, it was noted that certain weeks did not meet the predefined threshold for changes in the measured parameters. As a result, these weeks were included in the overall results but were not specifically highlighted in the figures. This implies that the corrective function was not applied during those weeks since the threshold for correction was not surpassed. While these weeks may not demonstrate significant changes or corrections, they are still considered in the evaluation process to provide a comprehensive assessment of the sensor performance.

As depicted in the figure, a notable observation is an evident increase in PM concentration when the RH level surpasses the threshold of 70%. This finding aligns with previous studies in the literature, reinforcing the clear correlation between high RH levels and elevated PM concentrations detected by LCS. Despite discovering that a threshold slightly higher than 70% resulted in improved performance with data, the decision was made to maintain a general threshold commonly used in other studies. This choice was motivated by the goal of developing a procedure that can be applied even in situations where no reference station is available. In any case, the selected threshold of 70% for the SPS30 sensors appears to effectively capture the occurrence of hygroscopicity events. Indeed, it is important to acknowledge that the sensitivity to humidity may vary among different sensors. This is particularly important when dealing with sensors from different manufacturers, as their designs and manufacturing processes can introduce additional variations in their performance. This variation in humidity sensitivity could explain the discrepancies observed between different sensors in their response to RH levels. Therefore, it becomes crucial to carefully evaluate and interpret the data from each sensor in the context of its specific characteristics and limitations.

Another significant observation from the figure is the clear cyclic pattern of humidity throughout the day. This cyclic pattern represents the regular fluctuations in humidity levels that occur over a day. These fluctuations can be influenced by various factors, including temperature variations, diurnal weather patterns, and human activities. It is important to note that taking a window size that is too small, such as just a few hours, may lead to the omission of important information regarding the classic behaviour of RH. By using a larger window size, encompassing a longer period, it becomes possible to capture and analyse the complete cyclic pattern of humidity (this aspect is presented also in sub- Section 4.3).

For a more comprehensive understanding of the corrective function's impact, an illustrative example is provided in Fig. 10. This example pertains to the spring period, specifically weeks 3 and 5, where LCS data is depicted before and after correction. Examining the scatter plots reveals that raw data collected under high relative humidity conditions have undergone reduction through the corrective function, resulting in improved alignment with the reference station data.

Another type of evaluation involves assessing how many times the LCS observations exceeds the maximum value recorded by the reference

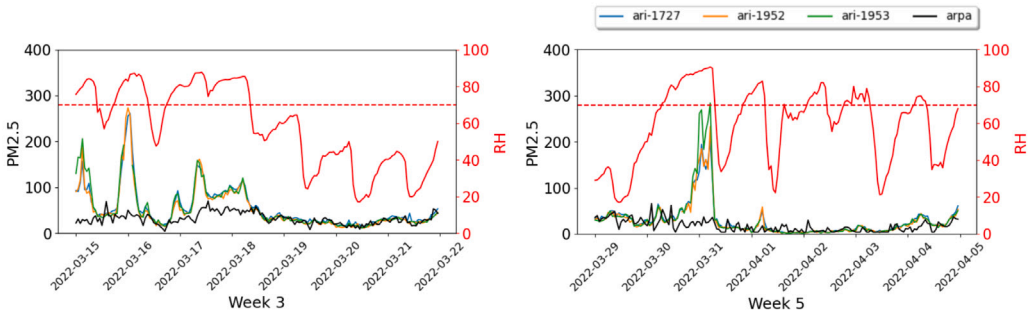

(a) Spring period raw data instance

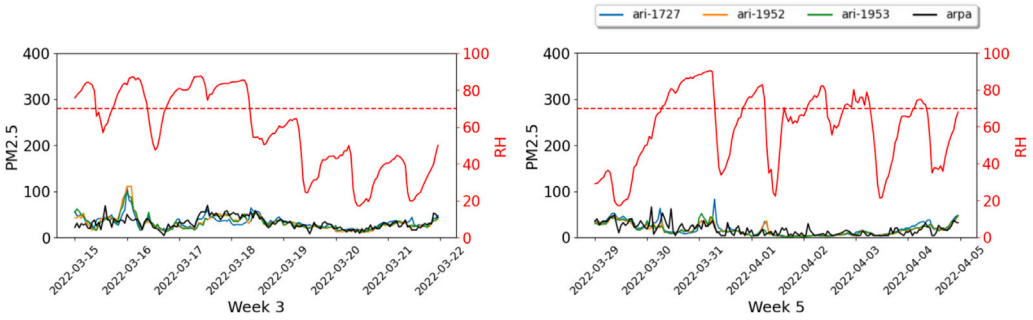

(b) Spring period corrected data instance

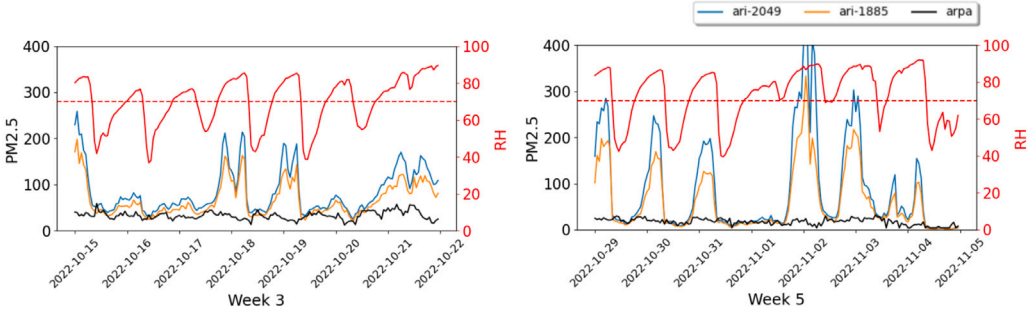

(c) Autumn period raw data instance

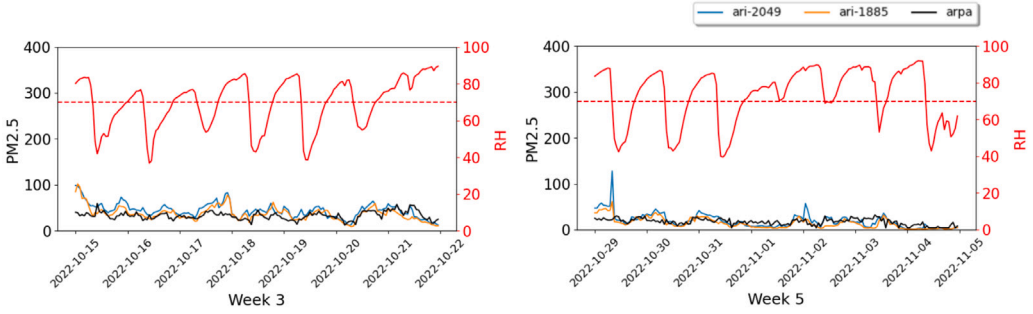

(d) Autumn period corrected data instance

Fig. 9. Performance overview of the MitH framework during spring and autumn periods, comparing original raw data with corrected data.

station in the period under examination (see Table 5). This evaluation can be performed even if the reference station data is not available on an hourly or daily basis. Instead, it is sufficient to have information regarding the maximum value detected and reported by the local agency.

4.5. Comparison with existing approaches

In this section, a comparative analysis between the approach presented in this study and existing methods proposed in the literature is conducted. Specifically, the corrective functions used in Streibl (2017) (Eqs. (2) and (3)) and Soneja et al. (2014) (Eqs. (4) and (5)) were considered. For the equations of *Chakrabarti* and *Richard*, fixed parameters were provided, and they were applied as such. However, in the analysis, each equation was re-fitted using the rolling window history procedure, enabling a more tailored and adaptable approach. This comparison allows for an assessment of the performance and effectiveness of MitH framework in comparison to existing techniques.

Regardless of whether fixed parameters were used or the equations were re-fitted, it is important to note that the pre-processing module's

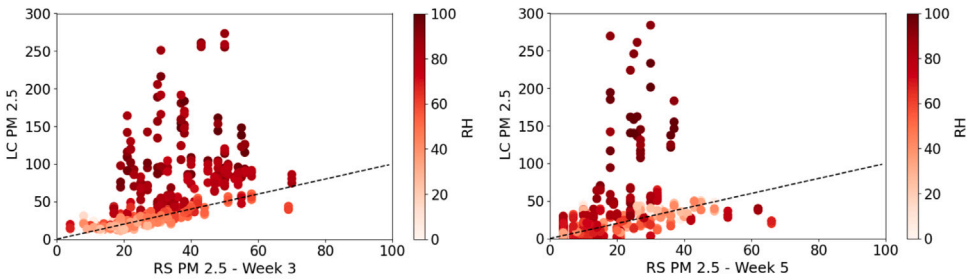

(a) Spring period raw data

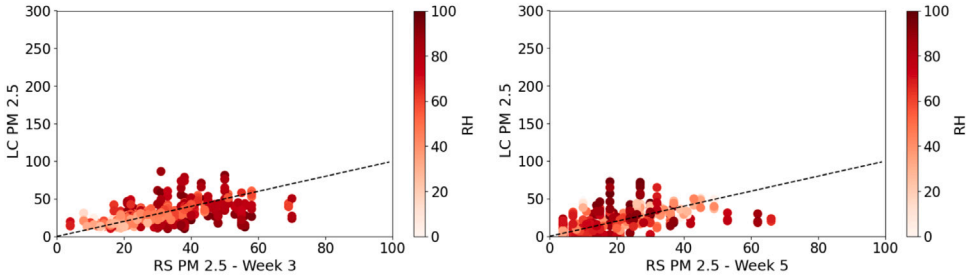

(b) Spring period corrected data

Fig. 10. Low-cost sensor data (y-axis) during the spring period, depicting the comparison with the reference station (x-axis) before and after correction. The colour gradient corresponds to relative humidity levels, and the black dotted line signifies perfect alignment.

Table 5
Percentage of LCS observations exceeding the maximum values detected by the reference station.

Sensor ID	Before correction	After correction
ari-1727	7.6%	2.6%
ari-1952	5.3%	0.8%
ari-1953	6.0%	1.1%
ari-1885	35.4%	7.3%
ari-2049	27.6%	6.3%

Table 6
Performance comparison of different corrective functions - Parameters: *window_size* of 1 day, optimization method correlation minimization, batch dimension of 1 day - the asterisk (*) indicates the use of fixed parameters as described in the original work.

Corrective function	Spring period			Autumn period		
	R^2	RMSE	NRMSE	R^2	RMSE	NRMSE
Combination	0.781	**11.157**	**0.506**	**0.636**	**12.010**	**0.563**
Hänel	0.716	12.676	0.575	0.494	14.846	0.696
Richard	0.723	13.496	0.612	0.530	14.980	0.702
Chakrabarti	0.741	12.496	0.567	0.536	15.081	0.707
Richard *	**0.793**	11.530	0.523	0.383	35.554	1.666
Chakrabarti *	0.787	11.987	0.543	0.395	31.661	1.484

step was always applied. The data underwent the three phases of module 2 (see Fig. 1), which involved statistical anomaly removal, data imputation, and smoothing. This ensured that the data used in the analysis were properly pre-processed and free from gross statistical anomalies, providing a reliable basis for comparison and evaluation of the different corrective functions.

The results in Table 6 provide an assessment of the performance of various corrective functions when evaluated against the reference station data. To ensure consistency in the evaluation, the LCS data were re-sampled at an hourly frequency to match the granularity of the reference station data. The *Combination* corrective function shows the best overall performance, with high R^2 values and low RMSE and NRMSE values. This indicates that the *Combination* function corrects for the influence of relative humidity on the sensor readings, leading to more accurate results.

In the spring period, *Chakrabarti* and *Richard*'s equations, with fixed parameters, also show relatively good performance, with R^2 values higher than the *Combination* function. However, in the autumn period, their performance is noticeably worse. This suggests that these equations may not be as effective in capturing the influence of relative humidity during different humidity conditions. This highlights the importance of considering the specific environmental context and optimizing the corrective function parameters accordingly. In this way, parameters are optimized for the location and context, but remain dynamic, and the approach could be exploited in each location, also without having a reference station co-located.

Hänel's corrective function shows the lowest performance among the evaluated functions, indicating that it may not adequately address the hygroscopicity issue caused by relative humidity.

4.5.1. Comparison with the Wiseair approach

The current study originally aimed to propose an alternative algorithm to the existing one used by Wiseair. In the existing approach, the pre-processing module involves masking PM values above a certain concentration threshold and filling them with the last available value. The algorithm then differentiates between summer and autumn months and applies a *Combination* corrective function with fixed parameters, chosen to use reference station data. Finally, regression is applied specifically for autumn observations. It is important to note that the existing algorithm relies on the use of a reference station for data correction, in fact, it focuses on removing the concentration of above-limit RH rather than cleaning it. This approach introduces complexity, as the regression model used during autumn is trained using data from a different period and location.

In comparing the performance of MitH to that of Wiseair's, the *single observation mode* was employed, tailored for real-time applications, allowing the correction of each observation upon arrival. The outcomes demonstrated notable performance enhancements with the MitH framework. Specifically, during the spring period, there was an increase in R^2 values by approximately 15%. In the autumn period, the improvement was even more remarkable, with an increase in R^2 values of around 30%. Correspondingly, RMSE and NRMSE values diminished.

5. Discussion

Based on the preceding discoveries, several noteworthy observations and implications can be discussed.

As anticipated, the comparison between the raw data and the corrected data reveals a significant impact of relative humidity on the PM concentration levels detected by LCS. When the RH exceeds a certain threshold, there is a noticeable increase in PM concentration. This observation emphasizes the importance of considering RH as a significant factor in data correction and analysis.

Additionally, the presence of an anomalous sensor, ari-1727, stands out in the analysis. This sensor consistently displays higher concentration levels compared to the other sensors. It is important to address such anomalies during the pre-processing, as they may not be directly related to hygroscopicity. The corrective function, in this case, does not adequately address this anomaly, and further investigation and pre-processing phases may be required to address the signal compromise.

When it comes to optimizing the parameters of the corrective function, the choice between including or excluding the observations to be corrected during the optimization module is critical. By including the observations, a more comprehensive context is considered, resulting in improved correction results. Conversely, excluding the observations may lead to a less effective correction, especially when RH levels exceed the threshold.

Furthermore, when comparing different measurement periods, such as spring and autumn, it becomes apparent that there are seasonal variations in PM concentration and RH levels. It is evident that these variations can impact the performance of the corrective function. The results show that the autumn period tends to yield worse performance in terms of R^2, RMSE, and NRMSE compared to the spring period. This can be attributed to long periods where RH exceed the threshold levels.

Additionally, the cyclic pattern of humidity throughout the day is an interesting observation. This cyclic pattern, which is likely influenced by temperature variations, diurnal weather patterns, and human activities, can contribute to fluctuations in the PM concentration levels. It is important to consider this cyclic pattern when determining the appropriate window size for the rolling window correction. Choosing a window size that aligns with the duration of the humidity cycle can help capture the relevant variations and improve the accuracy of the corrective function.

When comparing MitH with existing approaches, MitH demonstrates competitiveness. It is important to note that the goal is to develop a corrective function that does not rely on a ground truth, such as a reference station. In the literature, parameters for existing approaches are often found using regression techniques. In this study, corrective functions were optimized by minimizing the correlation between RH and PM, following the suggestion in Streibl (2017). Additionally, a technique involving the minimization of the distance between the original PM distribution under 70% RH and the distribution of data above 70% RH has been considered. Although this approach served as a starting point, it required further refinement. As a result, the corrected data using this approach performed better for the spring period but worse for the autumn period. The metric used for minimization was the standardized mean difference (SMD), and alternative approaches may yield better results. The decision was made not to pursue further exploration in this direction; however, it is important to recognize that alternative approaches could potentially provide better results.

Furthermore, an exploration was conducted to combine the *Combination* equation with the *Chakrabarti* equation. However, the results exhibited fluctuations, indicating that this combination might not be effective in addressing hygroscopicity.

Overall, these findings highlight the complexity and nuances involved in correcting LCS data for PM concentration. It underscores the importance of considering multiple factors, including RH, anomalies, seasonal variations, and optimization strategies, to improve the accuracy and reliability of the corrective function. Further research and refinement of the corrective algorithms are necessary to address these challenges and enhance the performance of LCS in monitoring and assessing air quality.

6. Conclusions

This paper introduces MitH, a framework designed to address hygroscopicity in the detection of particulate matter using laser scattering low-cost PM sensors. MitH reduces reliance on reference stations and enhances the accuracy of sensor data. The availability of open-source code enables comprehensive air quality assessment in various locations and facilitates the integration of LCS in interpolation techniques.

Unlike conventional approaches that use pre-trained models or ground truth data from reference stations, MitH focuses on developing context-specific and dynamic corrective functions. These functions are optimized based on the available data, making them adaptable to different contexts. Additionally, MitH includes data pre-processing and statistical anomaly removal.

The experimental results conducted in the urban area of Torino, Italy, demonstrate the effectiveness of MitH in enhancing sensor data accuracy. By considering the specific environmental context, MitH successfully mitigates the impact of hygroscopicity, leading to more precise PM measurements, evidenced by a 0.3 increase in R^2 during the autumn period.

Additionally, the study has shown that the use of a dynamic corrective function outperforms traditional approaches that rely on fixed parameters, especially during autumn when the environmental context seems to be more dynamic.

Future research in this domain aims to explore the integration of this procedure as an initial step, followed by the application of other techniques, including well-known machine learning and deep learning models, to further refine and adjust the data. The intention is to investigate the potential benefits of incorporating additional contextual information, such as meteorological data, geographical factors, elemental analysis, and temporal patterns, into the corrective process.

CRediT authorship contribution statement

Martina Casari: Conceptualization, Investigation, Methodology, Software, Validation, Visualization, Writing – original draft, Writing – review & editing. **Laura Po:** Conceptualization, Supervision, Validation, Writing – original draft, Writing – review & editing.

Declaration of competing interest

The authors declare that they have no known competing financial interests or personal relationships that could have appeared to influence the work reported in this paper.

Data availability

Data and code are available in a Git repository.

Acknowledgements

We would like to express our sincere appreciation to Wiseair and Arpa Torino for their valuable contributions to this study. The data collected and shared by both organizations have played a pivotal role in advancing our research and enhancing our understanding of air quality.

This paper will be published as part of the doctoral program within the "Dottorati di ricerca su tematiche green e dell'innovazione: nuove risorse dal PON Ricerca e Innovazione 14-20" funded by the Italian Ministry of Education, University and Research (D.M. n. 1061 del 10-8-2021).

References

Amegah, A.K., 2018. Proliferation of low-cost sensors. What prospects for air pollution epidemiologic research in Sub-Saharan Africa? Environ. Pollut. 241, 1132–1137. http://dx.doi.org/10.1016/j.envpol.2018.06.044, URL https://www.scopus.com/inward/record.uri?eid=2-s2.0-85049307474&doi=10.1016%2fj.envpol.2018.06.044&partnerID=40&md5=a97586f04dbb8e0bdb5c614824a481a1.

Amegah, A.K., Dakuu, G., Mudu, P., Jaakkola, J.J.K., 2022. Particulate matter pollution at traffic hotspots of Accra, Ghana: Levels, exposure experiences of street traders, and associated respiratory and cardiovascular symptoms. J. Expo. Sci. Environ. Epidemiol. 32 (2), 333–342. http://dx.doi.org/10.1038/s41370-021-00357-x, URL https://www.scopus.com/inward/record.uri?eid=2-s2.0-85109313048&doi=10.1038%2fs41370-021-00357-x&partnerID=40&md5=be2e6ddf77613fc6ff377724aadaffa8.

Apte, J.S., Messier, K.P., Gani, S., Brauer, M., Kirchstetter, T.W., Lunden, M.M., Marshall, J.D., Portier, C.J., Vermeulen, R.C., Hamburg, S.P., 2017. High-resolution air pollution mapping with Google street view cars: Exploiting big data. Environ. Sci. Technol. 51 (12), 6999–7008. http://dx.doi.org/10.1021/acs.est.7b00891, URL https://www.scopus.com/inward/record.uri?eid=2-s2.0-85021430709&doi=10.1021%2facs.est.7b00891&partnerID=40&md5=c45e5614282e169b0019aa34fc031232. All Open Access, Bronze Open Access.

ARPA-Torino, 2023. Torino rubino air quality monitoring station. URL http://www.sistemapiemonte.it/ambiente/srqa/stazioni/pdf/226.pdf. (Accessed 5 December 202).

Barkjohn, K.K., Gantt, B., Clements, A.L., 2021. Development and application of a United States-wide correction for PM2.5 data collected with the PurpleAir sensor. Atmos. Meas. Tech. 14 (6), 4617–4637. http://dx.doi.org/10.5194/amt-14-4617-2021, URL https://www.scopus.com/inward/record.uri?eid=2-s2.0-85108504291&doi=10.5194%2famt-14-4617-2021&partnerID=40&md5=99e967c18a19e54825ef0966ba8f82eb. All Open Access, Gold Open Access, Green Open Access.

Brusseleers, L., Nguyen, V.G., Vu, K.C., Dung, H.H., Somers, B., Verbist, B., 2023. Assessment of the impact of local climate zones on fine dust concentrations: A case study from Hanoi, Vietnam. Build. Environ. 242, http://dx.doi.org/10.1016/j.buildenv.2023.110430, URL https://www.scopus.com/inward/record.uri?eid=2-s2.0-85162088842&doi=10.1016%2fj.buildenv.2023.110430&partnerID=40&md5=e39b8de07f7bf2a01d8bdbd559c15a7b.

Campo, F., Franco, D., de Campos Santos, F., Blanco-Rodríguez, A., Garcia-Ramirez, A.R., Ratão, G., Hoinaski, L., 2023. CLEAN - Collaborative low-cost environmental and air-quality network. Environ. Model. Softw. 163, 105664. http://dx.doi.org/10.1016/j.envsoft.2023.105664, URL https://www.sciencedirect.com/science/article/pii/S1364815223000506.

Chakrabarti, B., Fine, P.M., Delfino, R., Sioutas, C., 2004. Performance evaluation of the active-flow personal DataRAM PM2.5 mass monitor (thermo Anderson pDR-1200) designed for continuous personal exposure measurements. Atmos. Environ. 38 (20), 3329–3340. http://dx.doi.org/10.1016/j.atmosenv.2004.03.007, URL https://www.scopus.com/inward/record.uri?eid=2-s2.0-2442428310&doi=10.1016%2fj.atmosenv.2004.03.007&partnerID=40&md5=e927f60840834e83eb643b8bdc09240c.

Chang, S.C., Lee, C.T., 2007. Secondary aerosol formation through photochemical reactions estimated by using air quality monitoring data in Taipei City from 1994 to 2003. Atmos. Environ. 41 (19), 4002–4017. http://dx.doi.org/10.1016/j.atmosenv.2007.01.040, URL https://www.scopus.com/inward/record.uri?eid=2-s2.0-34247882735&doi=10.1016%2fj.atmosenv.2007.01.040&partnerID=40&md5=8ca967dd40de9866df30c7a0eae9c04b.

Christakis, I., Moutzouris, K., Tsakiridis, O., Stavrakas, I., 2022. Barometric pressure as a correction factor for low-cost particulate matter sensors. In: IOP Conference Series: Earth and Environmental Science, vol. 1123, (no. 1), 012068. http://dx.doi.org/10.1088/1755-1315/1123/1/012068, URL https://www.scopus.com/inward/record.uri?eid=2-s2.0-85146635704&doi=10.1088%2f1755-1315%2f1123%2f1%2f012068&partnerID=40&md5=900951b02e92bd67e296cc784348d70d. All Open Access, Gold Open Access.

Coker, E.S., Buralli, R., Manrique, A.F., Kanai, C.M., Amegah, A.K., Gouveia, N., 2022. Association between PM2.5 and respiratory hospitalization in Rio Branco, Brazil: Demonstrating the potential of low-cost air quality sensor for epidemiologic research. Environ. Res. 214, http://dx.doi.org/10.1016/j.envres.2022.113738, URL https://www.scopus.com/inward/record.uri?eid=2-s2.0-85133626080&doi=10.1016%2fj.envres.2022.113738&partnerID=40&md5=6f5ace9958c9a8e2857142262947ff33.

Crilley, L.R., Shaw, M., Pound, R., Kramer, L.J., Price, R., Young, S., Lewis, A.C., Pope, F.D., 2018. Evaluation of a low-cost optical particle counter (Alphasense OPC-N2) for ambient air monitoring. Atmos. Meas. Tech. 11 (2), 709–720. http://dx.doi.org/10.5194/amt-11-709-2018, URL https://amt.copernicus.org/articles/11/709/2018/.

Crilley, L.R., Singh, A., Kramer, L.J., Shaw, M.D., Alam, M.S., Apte, J.S., Bloss, W.J., Hildebrandt Ruiz, L., Fu, P., Fu, W., Gani, S., Gatari, M., Ilyinskaya, E., Lewis, A.C., Ng'ang'a, D., Sun, Y., Whitty, R.C.W., Yue, S., Young, S., Pope, F.D., 2020. Effect of aerosol composition on the performance of low-cost optical particle counter correction factors. Atmos. Meas. Tech. 13 (3), 1181–1193. http://dx.doi.org/10.5194/amt-13-1181-2020, URL https://amt.copernicus.org/articles/13/1181/2020/.

Danek, T., Weglinska, E., Zareba, M., 2022. The influence of meteorological factors and terrain on air pollution concentration and migration: A geostatistical case study from Krakow, Poland. Sci. Rep. 12 (1), http://dx.doi.org/10.1038/s41598-022-15160-3, URL https://www.scopus.com/inward/record.uri?eid=2-s2.0-85133138138&doi=10.1038%2fs41598-022-15160-3&partnerID=40&md5=3f6fa0dcef51d71207f0f9b79a9e6cef. All Open Access, Gold Open Access, Green Open Access.

Day, D.E., Malm, W.C., 2001. Aerosol light scattering measurements as a function of relative humidity: A comparison between measurements made at three different sites. Atmos. Environ. 35 (30), 5169–5176. http://dx.doi.org/10.1016/S1352-2310(01)00320-X, URL https://www.sciencedirect.com/science/article/pii/S135223100100320X. Visibility, Aerosol and Atmospheric Optics.

Di Antonio, A., Popoola, O.A.M., Ouyang, B., Saffell, J., Jones, R.L., 2018. Developing a relative humidity correction for low-cost sensors measuring ambient particulate matter. Sensors (Switzerland) 18 (9), http://dx.doi.org/10.3390/s18092790, URL https://www.scopus.com/inward/record.uri?eid=2-s2.0-85052593655&doi=10.3390%2fs18092790&partnerID=40&md5=0d115ccaea4dfd0e2a23e461b4390b4e. All Open Access, Gold Open Access, Green Open Access.

Dimitriou, K., Stavroulas, I., Grivas, G., Chatzidiakos, C., Kosmopoulos, G., Kazantzidis, A., Kourtidis, K., Karagioras, A., Hatzianastassiou, N., Pandis, S.N., Mihalopoulos, N., Gerasopoulos, E., 2023. Intra- and inter-city variability of PM2.5 concentrations in Greece as determined with a low-cost sensor network. Atmos. Environ. 301, http://dx.doi.org/10.1016/j.atmosenv.2023.119713, URL https://www.scopus.com/inward/record.uri?eid=2-s2.0-85150251710&doi=10.1016%2fj.atmosenv.2023.119713&partnerID=40&md5=43ba7d7a87595dab0e4ef7a72c52e74e.

EEA, 2021. EU air quality directives. URL https://www.eea.europa.eu/themes/air/air-quality-concentrations/air-quality-standards.

Giordano, M.R., Malings, C., Pandis, S.N., Presto, A.A., McNeill, V., Westervelt, D.M., Beekmann, M., Subramanian, R., 2021. From low-cost sensors to high-quality data: A summary of challenges and best practices for effectively calibrating low-cost particulate matter mass sensors. J. Aerosol Sci. 158, http://dx.doi.org/10.1016/j.jaerosci.2021.105833, URL https://www.scopus.com/inward/record.uri?eid=2-s2.0-85110028282&doi=10.1016%2fj.jaerosci.2021.105833&partnerID=40&md5=7b2ea4963cf2f002da4888363acb4227. All Open Access, Green Open Access, Hybrid Gold Open Access.

Gurumurthy Ramachandran, G.C.P., Sexton, K., 2003. Characterizing indoor and outdoor 15 minute average PM 2.5 concentrations in urban neighborhoods. Aerosol Sci. Technol. 37 (1), 33–45. http://dx.doi.org/10.1080/02786820300889.

Hagan, D.H., Kroll, J.H., 2020. Assessing the accuracy of low-cost optical particle sensors using a physics-based approach. Atmos. Meas. Tech. 13 (11), 6343–6355. http://dx.doi.org/10.5194/amt-13-6343-2020, URL https://www.scopus.com/inward/record.uri?eid=2-s2.0-85097128902&doi=10.5194%2famt-13-6343-2020&partnerID=40&md5=bb5ef2ea3bed58d739bcf617bebe9c3c. All Open Access, Gold Open Access, Green Open Access.

Hill, D.J., Minsker, B.S., 2010. Anomaly detection in streaming environmental sensor data: A data-driven modeling approach. Environ. Model. Softw. 25 (9), 1014–1022. http://dx.doi.org/10.1016/j.envsoft.2009.08.010, URL https://www.scopus.com/inward/record.uri?eid=2-s2.0-77954860904&doi=10.1016%2fj.envsoft.2009.08.010&partnerID=40&md5=44a1dfc856bfcf78af92d3848a5923a3.

Hofman, J., Do, T.H., Qin, X., Bonet, E.R., Philips, W., Deligiannis, N., La Manna, V.P., 2022a. Spatiotemporal air quality inference of low-cost sensor data: Evidence from multiple sensor testbeds. Environ. Model. Softw. 149, http://dx.doi.org/10.1016/j.envsoft.2022.105306, URL https://www.scopus.com/inward/record.uri?eid=2-s2.0-85123866199&doi=10.1016%2fj.envsoft.2022.105306&partnerID=40&md5=0f11ad27f31faa613c19084b1c51866d.

Hofman, J., Nikolaou, M., Shantharam, S.P., Stroobants, C., Weijs, S., La Manna, V.P., 2022b. Distant calibration of low-cost PM and NO2 sensors; Evidence from multiple sensor testbeds. Atmos. Pollut. Res. 13 (1), http://dx.doi.org/10.1016/j.apr.2021.101246, URL https://www.scopus.com/inward/record.uri?eid=2-s2.0-85118846725&doi=10.1016%2fj.apr.2021.101246&partnerID=40&md5=1000bfe50c522915f41773e86e279abd.

Horsburgh, J.S., Reeder, S.L., Jones, A.S., Meline, J., 2015. Open source software for visualization and quality control of continuous hydrologic and water quality sensor data. Environ. Model. Softw. 70, 32–44. http://dx.doi.org/10.1016/j.envsoft.2015.04.002, URL https://www.scopus.com/inward/record.uri?eid=2-s2.0-84928548162&doi=10.1016%2fj.envsoft.2015.04.002&partnerID=40&md5=908a78af932aa8aea0496584074a571e. All Open Access, Hybrid Gold Open Access.

Int Panis, L., de Geus, B., Vandenbulcke, G., Willems, H., Degraeuwe, B., Bleux, N., Mishra, V., Thomas, I., Meeusen, R., 2010. Exposure to particulate matter in traffic: A comparison of cyclists and car passengers. Atmos. Environ. 44 (19), 2263–2270. http://dx.doi.org/10.1016/j.atmosenv.2010.04.028, URL https://www.scopus.com/inward/record.uri?eid=2-s2.0-77953086968&doi=10.1016%2fj.atmosenv.2010.04.028&partnerID=40&md5=16bddc8b6f4e7b02876d55f82d00b696.

Jayaratne, R., Liu, X., Thai, P., Dunbabin, M., Morawska, L., 2018. The influence of humidity on the performance of a low-cost air particle mass sensor and the effect of atmospheric fog. Atmos. Meas. Tech. 11 (8), 4883–4890. http://dx.doi.org/10.5194/amt-11-4883-2018, URL https://www.scopus.com/inward/record.uri?eid=2-s2.0-85052699528&doi=10.5194%2famt-11-4883-2018&partnerID=40&md5=85e3c565ccdc7ff03d4fb1cabf535790. All Open Access, Gold Open Access, Green Open Access.

Jin, X., Li, Z., Wu, T., Wang, Y., Cheng, Y., Su, T., Wei, J., Ren, R., Wu, H., Li, S., Zhang, D., Cribb, M., 2022. The different sensitivities of aerosol optical properties to particle concentration, humidity, and hygroscopicity between the surface level and the upper boundary layer in Guangzhou, China. Sci. Total Environ. 803, http://dx.doi.org/10.1016/j.scitotenv.2021.150010, URL https://www.scopus.com/inward/record.uri?eid=2-s2.0-85114149655&doi=10.1016%2fj.scitotenv.2021.150010&partnerID=40&md5=149975edf94d0dea5916995ba7c90387.

Jones, A.S., Jones, T.L., Horsburgh, J.S., 2022. Toward automating post processing of aquatic sensor data. Environ. Model. Softw. 151, http://dx.doi.org/10.1016/j.envsoft.2022.105364, URL https://www.scopus.com/inward/record.uri?eid=2-s2.0-85126538302&doi=10.1016%2fj.envsoft.2022.105364&partnerID=40&md5=7737aac00e86d40d7e3524e9e0de45b5. All Open Access, Green Open Access, Hybrid Gold Open Access.

Kelly, C., Fawkes, J., Habermehl, R., de Ferreyro Monticelli, D., Zimmerman, N., 2023. PLUME dashboard: A free and open-source mobile air quality monitoring dashboard. Environ. Model. Softw. 160, http://dx.doi.org/10.1016/j.envsoft.2022.105600, URL https://www.scopus.com/inward/record.uri?eid=2-s2.0-85145193073&doi=10.1016%2fj.envsoft.2022.105600&partnerID=40&md5=cbf708128fbca12d8bb97ba8f4dfe4a6. All Open Access, Hybrid Gold Open Access.

Kiesewetter, G., Schoepp, W., Heyes, C., Amann, M., 2015. Modelling PM2.5 impact indicators in europe: Health effects and legal compliance. Environ. Model. Softw. 74, 201–211. http://dx.doi.org/10.1016/j.envsoft.2015.02.022, URL https://www.scopus.com/inward/record.uri?eid=2-s2.0-84947024388&doi=10.1016%2fj.envsoft.2015.02.022&partnerID=40&md5=e61a0a5e0efacba1e5d7ace8a19b724d. All Open Access, Hybrid Gold Open Access.

Kosmidis, E., Syropoulou, P., Tekes, S., Schneider, P., Spyromitros-Xioufis, E., Riga, M., Charitidis, P., Moumtzidou, A., Papadopoulos, S., Vrochidis, S., Kompatsiaris, I., Stavrakas, I., Hloupis, G., Loukidis, A., Kourtidis, K., Georgoulias, A.K., Alexandri, G., 2018. HackAIR: Towards raising awareness about air quality in Europe by developing a collective online platform. ISPRS Int. J. Geo-Inf. 7 (5), http://dx.doi.org/10.3390/ijgi7050187, URL https://www.scopus.com/inward/record.uri?eid=2-s2.0-85047145586&doi=10.3390%2fijgi7050187&partnerID=40&md5=4a72b069b8dcc94383e1ca340e8b7c3c. All Open Access, Gold Open Access, Green Open Access.

Laquai, B., Kroseberg, B., 2021. Comparison of a computational method for correcting the humidity influence with the use of a low-cost aerosol dryer on a SDS011 low-cost PM-sensor. researchgate.

Li, Z., Guo, J., Ding, A., Liao, H., Liu, J., Sun, Y., Wang, T., Xue, H., Zhang, H., Zhu, B., 2017. Aerosol and boundary-layer interactions and impact on air quality. Natl. Sci. Rev. 4 (6), 810–833. http://dx.doi.org/10.1093/nsr/nwx117, arXiv:https://academic.oup.com/nsr/article-pdf/4/6/810/31567664/nwx117.pdf.

Manikonda, A., Zíková, N., Hopke, P.K., Ferro, A.R., 2016. Laboratory assessment of low-cost PM monitors. J. Aerosol Sci. 102, 29–40. http://dx.doi.org/10.1016/j.jaerosci.2016.08.010, URL https://www.sciencedirect.com/science/article/pii/S0021850216301021.

Molnár, A., Imre, K., Ferenczi, Z., Kiss, G., Gelencsér, A., 2020. Aerosol hygroscopicity: Hygroscopic growth proxy based on visibility for low-cost PM monitoring. Atmos. Res. 236, http://dx.doi.org/10.1016/j.atmosres.2019.104815, URL https://www.scopus.com/inward/record.uri?eid=2-s2.0-85076838451&doi=10.1016%2fj.atmosres.2019.104815&partnerID=40&md5=ff9713b79cfe4b336ed9f1e6e54a44a4. All Open Access, Hybrid Gold Open Access.

Owczarek, T., Rogulski, M., Czechowski, P.O., 2020. Assessment of the equivalence of low-cost sensors with the reference method in measuring PM10 concentration using selected correction functions. Sustainability (Switzerland) 12 (13), http://dx.doi.org/10.3390/su12135368, URL https://www.scopus.com/inward/record.uri?eid=2-s2.0-85088027028&doi=10.3390%2fsu12135368&partnerID=40&md5=fc0581a8877c2e8b34996a4433d92c32. All Open Access, Gold Open Access, Green Open Access.

Rajagopalan, S., Al-Kindi, S.G., Brook, R.D., 2018. Air pollution and cardiovascular disease: JACC state-of-the-art review. J. Am. Coll. Cardiol. 72 (17), 2054–2070. http://dx.doi.org/10.1016/j.jacc.2018.07.099, URL https://www.scopus.com/inward/record.uri?eid=2-s2.0-85054176359&doi=10.1016%2fj.jacc.2018.07.099&partnerID=40&md5=db0490fc0a88c9b8c8d1720e1bd83b62. All Open Access, Bronze Open Access.

Richards, L.W., Alcorn, S.H., McDade, C., Couture, T., Lowenthal, D., Chow, J.C., Watson, J.C., 1999. Optical properties of the San Joaquin Valley aerosol collected during the 1995 integrated monitoring study. Atmos. Environ. 33 (29), 4787–4795. http://dx.doi.org/10.1016/S1352-2310(99)00267-8, URL https://www.scopus.com/inward/record.uri?eid=2-s2.0-0033237877&doi=10.1016%2fS1352-2310%2899%2900267-8&partnerID=40&md5=927ed97606ebf85efbc26ab03c324b02.

Rogulski, M., Badyda, A., 2020. Investigation of low-cost and optical particulate matter sensors for ambient monitoring. Atmosphere 11 (10), http://dx.doi.org/10.3390/atmos11101040, URL https://www.scopus.com/inward/record.uri?eid=2-s2.0-85092690802&doi=10.3390%2fatmos11101040&partnerID=40&md5=59ea08103341b1b3b8b11ccee308cb73. All Open Access, Gold Open Access.

Russo, S., Lürig, M., Hao, W., Matthews, B., Villez, K., 2020. Active learning for anomaly detection in environmental data. Environ. Model. Softw. 134, 104869. http://dx.doi.org/10.1016/j.envsoft.2020.104869, URL https://www.sciencedirect.com/science/article/pii/S1364815220309269.

Sá, J.P., Alvim-Ferraz, M.C.M., Martins, F.G., Sousa, S.I., 2022. Application of the low-cost sensing technology for indoor air quality monitoring: A review. Environ. Technol. Innov. 28, 102551. http://dx.doi.org/10.1016/j.eti.2022.102551, URL https://www.sciencedirect.com/science/article/pii/S2352186422001432.

Samad, A., Mimiaga, F.E.M., Laquai, B., Vogt, U., 2021. Investigating a low-cost dryer designed for low-cost PM sensors measuring ambient air quality. Sensors (Switzerland) 21 (3), 1–18. http://dx.doi.org/10.3390/s21030804, URL https://www.scopus.com/inward/record.uri?eid=2-s2.0-85099886200&doi=10.3390%2fs21030804&partnerID=40&md5=5c7173fa093a33c8ae3a81e74a3ef3ba. All Open Access, Gold Open Access, Green Open Access.

Shi, J., Chen, F., Cai, Y., Fan, S., Cai, J., Chen, R., Kan, H., Lu, Y., Zhao, Z., 2017. Validation of a light-scattering PM2.5 sensor monitor based on the long-term gravimetric measurements in field tests. PLoS One 12 (11), http://dx.doi.org/10.1371/journal.pone.0185700, URL https://www.scopus.com/inward/record.uri?eid=2-s2.0-85033449574&doi=10.1371%2fjournal.pone.0185700&partnerID=40&md5=c1654ba774bb8f0c98e31d681b13cccf. All Open Access, Gold Open Access, Green Open Access.

Siciliano, T., Giua, R., Siciliano, M., Di Giulio, S., Genga, A., 2021. The morphology and chemical composition of the urban PM10 near a steel plant in Apulia determined by scanning electron microscopy. Source apportionment. Atmos. Res. 251, http://dx.doi.org/10.1016/j.atmosres.2020.105416, URL https://www.scopus.com/inward/record.uri?eid=2-s2.0-85098463824&doi=10.1016%2fj.atmosres.2020.105416&partnerID=40&md5=3cb9b7b5bb174eae23e86425a1e48d1f.

Skupin, A., 2013. Optische Und Mikrophysikalische Charakterisierung Von Urbanem Aerosol Bei (Hoher) Umgebungsfeuchte (Ph.D. thesis). Verlag nicht ermittelbar.

Soneja, S., Chen, C., Tielsch, J.M., Katz, J., Zeger, S.L., Checkley, W., Curriero, F.C., Breysse, P.N., 2014. Humidity and gravimetric equivalency adjustments for nephelometer-based particulate matter measurements of emissions from solid biomass fuel use in cookstoves. Int. J. Environ. Res. Public Health 11 (6), 6400–6416. http://dx.doi.org/10.3390/ijerph110606400, URL https://www.scopus.com/inward/record.uri?eid=2-s2.0-84902988962&doi=10.3390%2fijerph110606400&partnerID=40&md5=1f20e0f57712ad3713ad14d6744f7e2d. All Open Access, Gold Open Access, Green Open Access.

Sousan, S., Regmi, S., Park, Y.M., 2021. Laboratory evaluation of low-cost optical particle counters for environmental and occupational exposures. Sensors 21 (12), http://dx.doi.org/10.3390/s21124146, URL https://www.scopus.com/inward/record.uri?eid=2-s2.0-85108010526&doi=10.3390%2fs21124146&partnerID=40&md5=1a1c6f506e69904dfd90ab747f062251. All Open Access, Gold Open Access, Green Open Access.

Streibl, N., 2017. Influence of humidity on the accuracy of low-cost particulate matter sensors. Techn. Ber. Tech. Rep. DOI 10.

Verhoeven, J.I., Allach, Y., Vaartjes, I.C.H., Klijn, C.J.M., de Leeuw, F.-E., 2021. Ambient air pollution and the risk of ischaemic and haemorrhagic stroke. Lancet Planet. Health 5 (8), e542–e552. http://dx.doi.org/10.1016/S2542-5196(21)00145-5, URL https://www.sciencedirect.com/science/article/pii/S2542519621001455.

WHO, et al., 2021. WHO Global Air Quality Guidelines: Particulate Matter (PM2. 5 and PM10), Ozone, Nitrogen Dioxide, Sulfur Dioxide and Carbon Monoxide: Executive Summary. World Health Organization.

Xue, Y., Wang, L., Zhang, Y., Zhao, Y., Liu, Y., 2022. Air pollution: A culprit of lung cancer. J. Hazard. Mater. 434, 128937. http://dx.doi.org/10.1016/j.jhazmat.2022.128937, URL https://www.sciencedirect.com/science/article/pii/S0304389422007269.

Zafra-Pérez, A., Boente, C., de la Campa, A.S., Gómez-Galán, J., de la Rosa, J., 2023. A novel application of mobile low-cost sensors for atmospheric particulate matter monitoring in open-pit mines. Environ. Technol. Innov. 29, http://dx.doi.org/10.1016/j.eti.2022.102974, URL https://www.scopus.com/inward/record.uri?eid=2-s2.0-85143680168&doi=10.1016%2fj.eti.2022.102974&partnerID=40&md5=028063899e3b2d602a5ed439236996cb. All Open Access, Gold Open Access, Green Open Access.

Zhivkov, P., 2021. Optimization and evaluation of calibration for low-cost air quality sensors: Supervised and unsupervised machine learning models. In: Proceedings of the 16th Conference on Computer Science and Intelligence Systems, FedCSIS 2021. pp. 255–258. http://dx.doi.org/10.15439/2021F95, URL https://www.scopus.com/inward/record.uri?eid=2-s2.0-85117793346&doi=10.15439%2f2021F95&partnerID=40&md5=2f0e02da6b0d78aaa6523df4f48308c9. All Open Access, Gold Open Access.

Zhu, F., Ding, R., Lei, R., Cheng, H., Liu, J., Shen, C., Zhang, C., Xu, Y., Xiao, C., Li, X., Zhang, J., Cao, J., 2019. The short-term effects of air pollution on respiratory diseases and lung cancer mortality in Hefei: A time-series analysis. Respir. Med. 146, 57–65. http://dx.doi.org/10.1016/j.rmed.2018.11.019, URL https://www.sciencedirect.com/science/article/pii/S0954611118303901.

Zusman, M., Schumacher, C.S., Gassett, A.J., Spalt, E.W., Austin, E., Larson, T.V., Carvlin, G., Seto, E., Kaufman, J.D., Sheppard, L., 2020. Calibration of low-cost particulate matter sensors: Model development for a multi-city epidemiological study. Environ. Int. 134, http://dx.doi.org/10.1016/j.envint.2019.105329, URL https://www.scopus.com/inward/record.uri?eid=2-s2.0-85075537069&doi=10.1016%2fj.envint.2019.105329&partnerID=40&md5=65328ba8c19e6934681775e09eba6b6c. All Open Access, Gold Open Access, Green Open Access.